*Association of Metallurgical Engineers of Serbia* *Scientific paper*
*AMES* *UDC: 621.746.2:621.643.23*

# PROPERTIES OF HEAT TREATED CENTRIFUGALLY CAST HIGH STRENGTH STEEL TUBES

Boris Katavić [1*], Bojan Gligorijević[1], Zoran Odanović[2], Mile Djurdjević[3]

[1]*Institute Goša, Milana Rakića 35, Belgrade, Serbia,*
[2]*IMS Institute, Bulevar Vojvode Mišića 43, Belgrade, Serbia*
[3]*Nemak Linz, Zeppelinstrasse 24, 4030 Linz, Austria*

*This paper was previously presented at*
*4th International Conference Processing and Structure of Materials*
*held on Palic, Serbia May 27- 29, 2010*

## Abstract

The effects of heat treatment on structural and mechanical properties of the centrifugally cast CrMo and CrMoNb high strength steel tubes of different diameters and wall thicknesses are presented in this paper. Centrifugal casting process was performed at mould rotation speeds ranging from 1320 to 1562 rpm. Specimens were homogenized at 1323 K, austenitized at 1143 K, quenched and tempered between 473 K and 923 K. The results of tensile and Charpy impact testing show intensive increase in ductility properties and impact energy at temperatures above 823 K, while strength decreases gradually with tempering temperature. Variations of the mechanical properties with tempering temperature were modeled by means of polynomial functions.
*Key words: Centrifugal casting, high strength steel tubes, heat-treatment, micro-structure, mechanical properties, modeling*

## Introduction

Centrifugal casting (CC) is a casting technology wherein molten metal crystallizes under the dominant influence of the centrifugal force ($F_c$), which occurs during the rotation of the mould. As a result of this action, CC products are of higher density in comparison to those obtained by use of standard casting methods. Magnitude of $F_g$ is defined by the gravitational factor (coefficient) k, which is given as *centrifugal* to gravitational *force ratio, i.e.* $k = F_c/F_g$. Parameters of the centrifugal casting process, like mould rotation speed (n), casting temperature ($T_1$) and casting speed ($v_1$), have **a** strong influence on the final quality of as-cast products [1-5]. The mould rotation speed has a significant impact on structural formation mechanisms in the radial direction [1, 2,

* Corresponding author: Boris Katavić, boris.katavic@institutgosa.rs

6, 7]. In general, the centrifugal casting of steel products was significantly less applied than casting of grey iron and non-ferrous metal based products [1 - 7]. References concerning the CC of CrMo and CrMoNb high strength steel tubes are not found in literature. Our previous investigations have included analysis of distribution of chemical elements, the type and distribution of structure and nonmetallic inclusions in as-cast CC CrMo and CrMoV high strength steel tubes of different diameters and wall thicknesses [6-7]. The aim of this study is to examine the effects of the heat treatment on mechanical and structural properties of CC Cr-Mo and Cr-Mo-Nb high strength steel tubes of different diameters and wall thicknesses. The attention will be focused on effects caused by existing differences in starting structural properties of these steel tubes and effects caused by Nb doping of CrMo high strength steel tubes.

## Experimental Part

*Materials*

The average chemical composition of CrMo and CrMoNb high strength steel tubes is given in Table 1. Molten steel, after treatment in the medium-frequency induction furnace of 1000kg/1MW, was poured into the steel moulds of the centrifugal machines, with horizontal rotation axis, when casting conditions were established (Table 2). Before liquid metal was introduced, steel moulds were dry-coated with fine granulated $Al_2O_3$ and formaldehyde pitch. The tubes C1 and C2 were cast in the steel mould of dimensions (∅264/∅182×2100) mm and the tube A in the steel mould of dimensions (∅260/∅165×1405) mm. The chemical composition of castings was determined by using standard spectrophotometric method. Leco apparatus was used to determine the oxygen and nitrogen content. The annular samples (rings) were obtained by cutting from middle of the CC tubes. Subsequently, rings were cut in ring segments. Heat treatment was performed on C1, C2 and A prismatic-like samples that were taken from ring segments. All types of prismatic-like samples were of similar dimensions. Test specimens of standards dimensions for microstructural characterization and mechanical testing were produced by machining of heat-treated prismatic-like samples.

*Table 1. Average chemical compositions of Cr-Mo and CrMoNb centrifugally cast steel tubes*

| Steel | Chemical composition [wt. %] | | | | | | | | | | | | |
|---|---|---|---|---|---|---|---|---|---|---|---|---|---|
| Mark | C | Mn | Si | S | P | Cr | Mo | Nb | Ni | Cu | Al | O | N |
| CrMo | 0.20 | 0.60 | 0.44 | 0.028 | 0.032 | 1.25 | 0.15 | | 0.160 | 0.140 | 0.080 | 0.0038 | 0.014 |
| CrMoNb | 0.24 | 0.55 | 0.45 | 0.030 | 0.033 | 1.15 | 0.15 | 0.11 | 0.090 | 0.090 | 0.050 | 0.0350 | 0.025 |

*Table 2. The casting conditions of the CrMo and CrMoNb centrifugally cast steel tubes $T_k$ - Mould temperature [K]; $T_l$- Pouring temperature [K]; $\tau_l$- Pouring time; $\tau_h$-Cooling time; $n_k$- Mould rotation speed, k = $F_c$/Fg-Gravitational factor (coefficient); $F_c$-Centrifugal force; $F_g$-Gravity force; $d_s$-Outside tube diameter; $\delta$ - Tube wall thickness ; $\delta_k$ - Mould wall thickness; l - Tube length*

| Steel | Cast | $T_k$ K | $T_l$ K | $\tau_l$ s | $\tau_h$ s | $n_k$ rpm | k | $d_s$ mm | $\delta$ mm | l mm | $\delta_k/\delta$ |
|---|---|---|---|---|---|---|---|---|---|---|---|
| CrMo | C1 | 423 | 1863 | 35 | 700 | 1562 | 102 | 176 | 50 | 2000 | 0.82 |
| CrMo | C2 | 423 | 1863 | 35 | 600 | 1315 | 101 | 172 | 33 | 2000 | 1.24 |
| CrMoNb | A | 423 | 1903 | 15 | 390 | 1320 | 107 | 155 | 22.5 | 1400 | 2.11 |

*Heat treatment*

The samples were treated in a heat-resistant furnace. Fluctuations in furnace temperature were approximately ± 5 K. The samples C1, C2 and A were annealed at 1323 K for 60 minutes, cooled down to 573 K in furnace and air-cooled down to room temperature. After, they were austenitized at 1143 K for 60 minutes and subsequently oil-quenched. During the last stage of heat treatment A samples were tempered at 573 K and between (773 – 973) K in temperature steps of 50 K. C1 and C2 samples were tempered between (473 – 773) K in steps of 100 K, and between (773 – 923) K in steps of 50 K. Tempering time was 60 min, heating rate 4-5 K/min, and the oil-cooling temperature 293 K.

*Mechanical testing*

The tensile tests were performed according to SRPS EN 10002-1 on the round specimens with the gage length of 30 mm and diameter of 6 mm. The tensile tests were carried out on an Instron M8033 tensile machine of 100 kN load capacity with a tension rate of $1.2 \times 10^{-5}$ m/s. The impact energy was determined according to SRPS EN 10045-1 standard on a Tinius Olsen Charpy pendulum of 348 Nm equipped with a Teletronix 51-13 oscilloscope. The dimensions of the U notched specimens were 10x10x55mm. The Vickers hardness HV30 was measured on the sample cross-sections by the Wolpert-Dia testor 2Rc-type equipment. At least three tensile tests were carried out, whereas hardness measurements were performed on each specimen.

*Structural analysis*

The specimens were grinded, polished and subsequently etched with 3% Nital solution whereupon the microstructure was analyzed with light microscope (LM). The

structure of tempered samples (at 573 K) of tube A was also observed with transmission electron microscope (TEM) JEOL 120X and analyzed by using the electron diffraction analysis (ED).

## Results and Discussion

Figs. 1-3 show changes in mechanical properties of C1, C2 and A test specimens, tempered in the temperature range from 473 to 923 K and from 773 to 973 K.

Equations describing mechanical behavior of tempered specimens C1 and C2 (Fig. 1 and 2) are given in Tables 3 and 4, respectively. Fitting procedure has shown that polynomial function of the 4$^{th}$ order is in the best agreement with experimentally obtained results. Fitting was performed by using the Levenberg-Marquardt iteration method. Fitting of experimental results obtained from specimens A was not performed because, unlike the C1 and C2, the tempering of A samples was not performed in a sufficient temperature range.

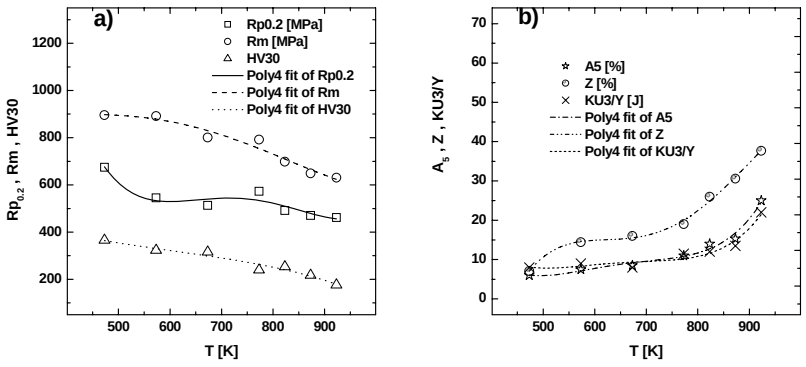


*Fig. 1. Effects of tempering on mechanical properties of C1 samples: a) the yield strength ($R_{p0.2}$), the tensile strength ($R_m$), and the hardness (HV); b) the elongation ($A_5$), the area reduction (Z), the impact energy in radial (y-direction) – KU3/Y.*

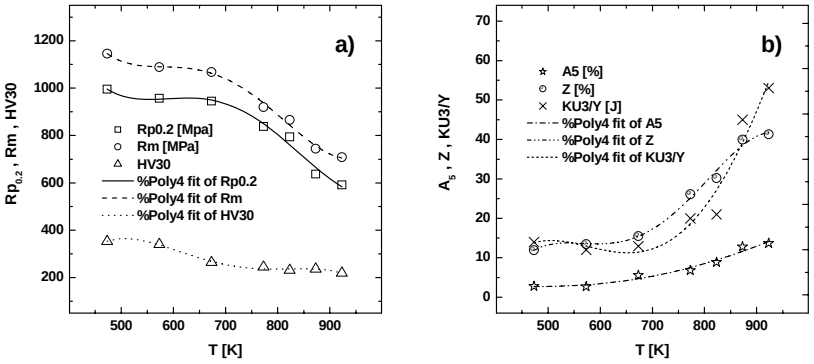


*Fig. 2. Effects of tempering on mechanical properties of C2 samples: a) the yield strength ($R_{p0.2}$), the tensile strength ($R_m$), and the hardness (HV); b) the elongation ($A_5$), the area reduction (Z), the impact energy in radial (y-direction) – KU3/Y.*

The LM photomicrographs of tempered specimens C1, C2 and A are shown in Figs. 4 - 6. Characteristic results obtained after ED and TEM of A specimen tempered at 573 K are presented in Fig. 7 a) and b), respectively. C1 and C2 tubes are materials of the similar grade (Table 1). However, having different wall thicknesses (Table 2), they have suffered different cooling conditions during the solidification, which has resulted in different structural properties after centrifugal casting [5-7]. C1 tubes with thicker walls, in comparison to that of C2, have had structure that is more inhomogeneous in as-cast state [6, 7]. Inherited structural differences of C1 and C2 had a significant impact on their structural and mechanical properties after quenching and tempering.

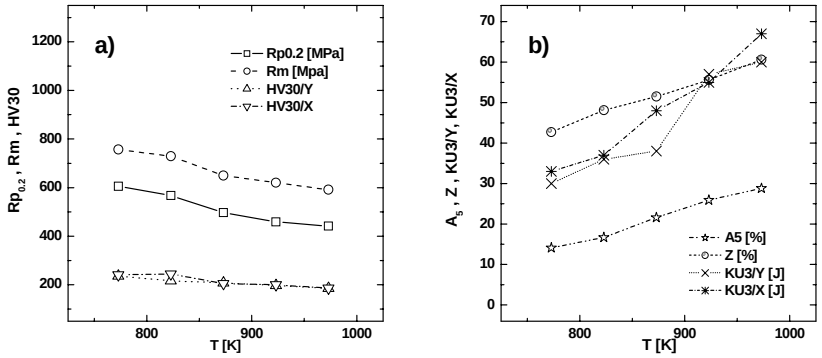


*Fig. 3. Effects of tempering on mechanical properties of A samples: a) the yield strength ($R_{p0.2}$), the tensile strength ($R_m$), the hardness in radial (y-direction) – HV30/Y and axial (x-direction) – (HV30/X); b) the elongation ($A_5$), the area reduction (Z), the impact energy in radial (y-direction) – KU3/Y and axial (x-direction) – KU3/X.*

*Table 3. Regression equations of mechanical properties of the tempered C1 samples*

| Property* | $Chi^2$/DoF | $R^2$ |
|---|---|---|
| $R_{P0.2} = 15840 - 85.516*T + 0.17657*T^2 - 0.00016*T^3 + 5.3059E\text{-}8*T^4$ [MPa] | 1432.8 | 0.913 |
| $R_m = 1270.5 - 3.2595*T + 0.01010*T^2 - 0.00001*T^3 + 5.2644E\text{-}8*T^4$ [MPa] | 1461.0 | 0.958 |
| $HV30 = 658.22 - 0.86119*T + 0.00028*T^2 - 8.6665E\text{-}7*T^3 - 8.3329E\text{-}10*T^4$ | 535.5 | 0.960 |
| $A_5 = 421.330 - 2.6832*T + 0.00638*T^2 - 6.6418E\text{-}6*T^3 - 2.5683E\text{-}9*T^4$ [%] | 2.334 | 0.981 |
| $Z = - 869.93 + 5.0111*T - 0.01047*T^2 + 9.5036E\text{-}6*T^3 - 3.1296E\text{-}9*T^4$ [%] | 1.440 | 0.996 |
| $KU3/Y = + 352.29 - 2.2179*T - 0.00528*T^2 - 5.5229E\text{-}6*T^3 + 2.1476E\text{-}9*T^4$ [J] | 3.260 | 0.955 |

*Table 4. Regression equations of mechanical properties of the tempered C2 samples*

| Property | $Chi^2$/DoF | $R^2$ |
|---|---|---|
| $R_{P0.2} = 14344 - 80.9424*T + 0.17985*T^2 - 0.00017*T^3 + 6.0513E\text{-}8*T^4$ [MPa] | 1023.9 | 0.987 |
| $R_m = 15614 - 88.879*T + 0.20091*T^2 - 0.00002*T^3 + 7.0932E\text{-}8*T^4$ [MPa] | 475.7 | 0.995 |
| $HV30 = -8869.56 + 55.8922*T - 0.12322*T^2 + 0.00012*T^3 - 4.0873E\text{-}10*T^4$ | 55.15 | 0.994 |
| $A_5 = -3.38328 + 0.06770*T - 0.00022*T^2 + 2.6934E\text{-}7*T^3 - 9.4891E\text{-}11*T^4$ [%] | 1.680 | 0.971 |
| $Z = -958.13 + 6.09616*T - 0.01047*T^2 + 0.00001*T^3 - 5.1324E\text{-}9*T^4$ [%] | 3.532 | 0.992 |
| $KU3/Y = -564.82 + 3.4600*T - 0.00741*T^2 + 6.6173E\text{-}6*T^3 - 2.0225E\text{-}9*T^4$ [J] | 39.52 | 0.952 |

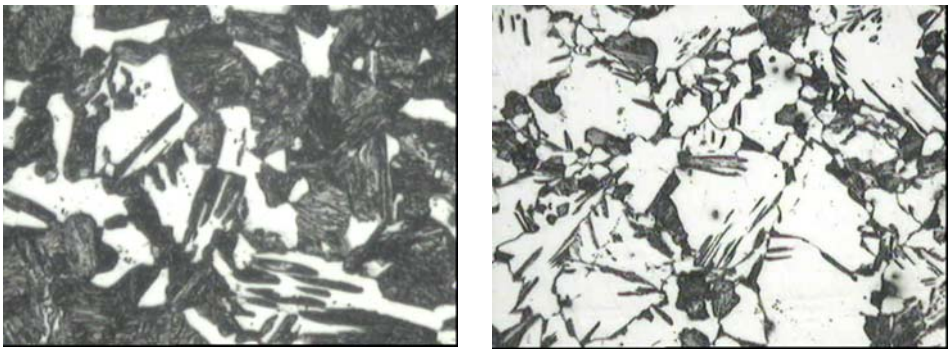

*a) ×500* *b) ×200*

*Fig. 4. LM. Microstructure of the heat treated centrifugally cast steel tube C1tempered at: a) 473K; b) 923K; tempering time – 60 min; oil-cooled; etched by the 3% Nital reagent.*

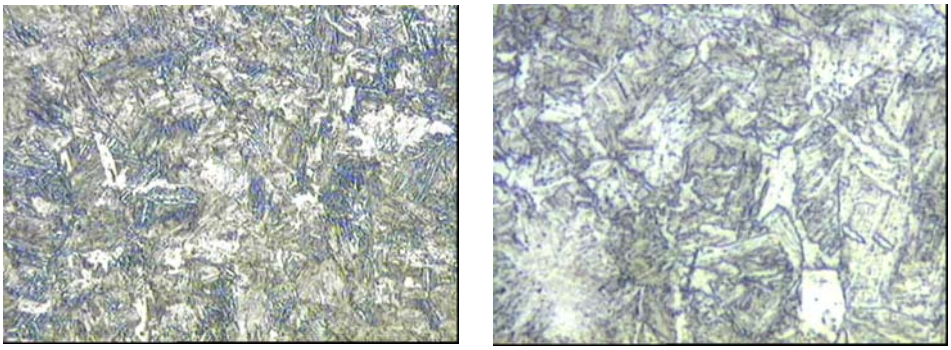

*a) ×200* *b) ×200*

*Fig. 5. LM. Microstructure of the heat treated centrifugally cast steel tube C2 tempered at: a) 473K; b) 923K; tempering time – 60 min; oil-cooled; etched by the 3% Nital reagent.*

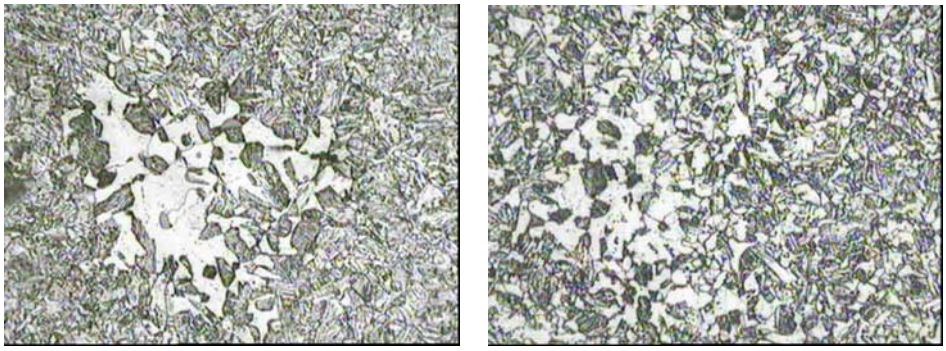

*a) ×200* *b) ×200*

*Fig. 6. LM. Microstructure of the heat treated centrifugally cast steel tube A tempered at: a) 773K; b) 973K; tempering time – 60 min; oil-cooled; etched by the 3% Nital reagent*

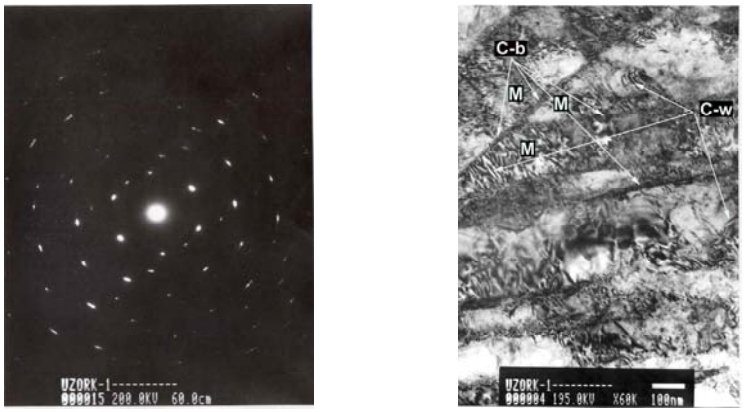


*a)* *b)*

*Fig. 7 ED a) and TEM b) images of specimens A tempered at 573 K; Carbide and/or carbonitride precipitates between (C-b) and within (C-w) martensitic lamellae; M – martensitic lamella.*

During tempering roughly up to 673 K, no significant changes in all mechanical properties are observed in C1 and C2 test specimens (Fig. 1 and 2). The possible reason can be the relative structural stability of metastable martensitic structure due to a slow diffusion of carbon and much lower diffusion of other alloying elements [8-13]. In tempering range up to 673 K diffusion is probably causing only the formation of fine-dispersed carbide particles i.e. the slow decomposition of martensite. The only general difference in mechanical properties between C1 and C2 is higher level in strength and impact energy in the case of C2.

Tempering above 673 K has caused significant changes in mechanical properties of both test specimens (C1 and C2), especially in case of C2. Generally, the diffusion of carbon and carbide-forming elements above 673 K is faster and it is probably

responsible for progressive precipitation and coagulation of carbides, in this way noticeably affecting the mechanical properties above 673 K. In other words, instability of martensitic structure above 673 K is significant. Due to differences in inherited structure properties, the martensite of C2 was probably more saturated with carbon than that of C1. For this reason, after quenching, the C2 had probably higher dislocation density, which is why it had the higher strength level and noticeably faster drop in strength with increasing the tempering temperature, in contrast to C1. C1 had probably more dislocation free zones than C2 and that is why the tempering had smaller effect on its strength level above 673K [8, 9, 11, 12]. In addition, more disperse structure observed in C2 (Fig 5b) than that of C1 (Fig. 4b) means that higher fraction of grain boundary area was present in the bulk of C2 meaning that more locations for precipitation and coagulation of carbides were available. Tempering above 673 K up to 923 K considerably reduced the fraction of martensite. In contrast, the ferrite fraction is increased in both samples, C1 and C2. More precisely, the general structure consists of ferrite, small amounts of pearlite, tempered martensite and carbides (Fig. 4b and 5b). The bainite presence is observed in the structure of samples C2. Despite greater structural instability above 673 K and greater changes in mechanical properties, C2 samples have preserved higher level of strength in comparison to that of C1.

Test specimens of tube A show slow gradual drop in yield and tensile strenght and hardness in radial (y-axis) and in axial (x-axis) direction (Fig. 3a). Properties of ductility i.e. elongation and reduction of area as well as toughness i.e. impact energy show slow linear increase with tempering temperature (Fig. 3b). There are no significant difference in impact energy observed in specimens sampled in radial and axial direction. It can be noticed that C2 and A tubes had an approximately similar chemical composition (Table 1). Having the smaller wall thickness (Table 2), the A tubes have suffered faster cooling during solidification. This implies that A tubes had a more stressed and disperse structure in as-cast state than that of C2 and especially that of C1. Normally, more stressed and disperse martensitic structure leads to a noticeable decomposition of martensite and precepitation of carbides along the grain boundaries and dislocations above 673 K. However, such drop in strength properties in A samples was not observed (Fig. 3) like in case of C2 (Fig. 2). Unlike C2, A samples contained certain amount of Nb (Table 1). The main role of Nb is formation of fine-dispersed carbide and/or carbonitride particles along the grain boundaries and dislocations preventing the formation of other undesirable carbide forms e.g. Cr-based carbides [10-13]. In this way, Nb addition has enabled structural stability of A samples in terms of maintaining the fine-dispersed structure up to the highest tempering temperatures applied in this work. Fig. 7b show presence of lath martensite in the bulk of A samples tempered at 573 K. From this figure, dark phases can be observed, which are present between the boundaries of martensitic lamellas (C-b) and within lamellas (C-w). Fig 7a shows ring-like electron diffraction pattern, which is probably the result of differently oriented martensitic lamellas (M in Fig. 7b). Around reflections that probably come from lath martensite in Fig 7a can be noticed an additional reflections, which probably come from Nb-based carbides/carbonitrides and/or Fe/Cr-based complex carbides (Fig. 7b). It can be concluded that precipitation of fine-dispersed Nb-based carbide and/or carbonitride particles has probably taken place along the grain boundaries (C-b) and dislocations (C-w). Existence of these particles probably retards the diffusion of carbon and carbide-forming elements along the grain boundaries and dislocations thus

preventing the precipitation and coagulation of undesirable forms of carbides. In this way, fine-dispersed microstructure (structural stability) is maintained with addition of Nb to the highest tempering temperatures as well as high level and stability of mechanical properties (Fig. 3). Additionally, C-w precipitations (Fig. 7b) probably prevent to the certain amount rearrangement of dislocations towards the grain boundary areas i.e. prevent structural recovery, unlike in the case of C2. Microstructure of samples of the tube A, tempered at 773 K is composed of martensite, bainite and disperse carbides and/or carbonitrides (Fig. 6a). The effect of Nb addition on structural properties can be clearly seen by comparing the photomicrographs shown in Fig. 5b and Fig. 6b. It is obvious that the microstructure of C2 and A samples, tempered at 923 K and 973 K, respectively, consists of ferrite, small amounts of pearlite, disperse carbides. In addition, it is obvious that A samples had more disperse structure probably due to addition of Nb and formation of its carbides and/or carbonitrides.

## Conclusions

In range of tempering up to roughly 673 K relative stability in mechanical properties of C1 and C2 tempered samples is probably due to a slow decomposition of martensite. Generally, C2 exibits higher level of strenght, ductility and toughness properties than C1 which is probably connected to differences in inherited (as-cast) properties. Above 673 K changes in their (C1 and C2) mechanical properties are observed. Faster diffusion processes and existence of higher dislocation density (more stressed martensite structure after quenching) in the bulk of C2 are probable reasons for higher structural instability and faster drop in strength and increase in ductility and impact energy in comparison to that of C1 above 673 K. Unlike Nb-free samples (C2), Nb-containing samples (A) have demonstrated greater structural stability and higher level of mechanical properties at highest tempering temperatures that were applied in this work. Presence of Nb-based carbides and/or carbonitrides probably delays martensite to ferrite transition i.e. structural recovery and recrystallization of ferrite.

*Acknowledgements*

The Ministry of Science of Republic of Serbia supported publication of this paper in completion of project 34028. We gratefully acknowledge technical support provided from research staff working at Laboratory of Military-Technical Institute in Belgrade, Serbia.

## References

[1] G. S. Mirzojan i dr., Litejnoje proizvostvo, 5 (1985) 16.
[2] E. O. Paton i dr., Elektrošljakovaj tigeljnaj plavka i razlivka metala, Naukova Dumka, Kiev (1988) 100.
[3] E. K. Ivanko, Litejnoje Proizvodstvo, 6 (1989) 31.
[4] Read – Hill R. E., Physical Metallurgy, D. Van Nostrand Co, New York 1973.
[5] A. M. Dobrijnin, G. S. Mirzojan, Litejnoje Proizvodstvo, 3 (1990) 14

[6] B. Katavić, Chemical and Structural Inhomogeneity of the Centrifugally Cast Steel Tubes, 4th Balkan Conference on Metallurgy, Proceedings, Zlatibor, 27-29 September, 2006, 631-636.
[7] B. Katavić, Z. Odanović, Analysis of nonmetallic inclusions Distribution and Microstructure in Centrifugally Cast Steel Pipes, 3th International Conference, Deformation processing and Structure of Materials, Proceedings, Zlatibor, 20-22 September, 2007, 207-214.
[8] M. A. Valter i dr., Vlijanija otpuska posle obkatki rolikani na fiziko mehaničeskija svojstva stali, Mitom No. 4, Moskva, 1979
[9] B. Katavić, S. Matijašević, S. Marković, M. Mičević, 3th. Yugoslavian Conference on Casting, Proceedings, 1987
[10] V. Ollialinen, M. Sulonen, Wire, 10 (1978) 190
[11] I. I. Novikov, Teorija termičeskoj obrabotke metalov, Moskva, 1978
[12] J. J. Matrosov, I. P. Bardin, Metalovedenije i termičeskaja obrabotka metalov, 11 (1984) 13.
[13] B. Katavić, S. Matijašević, S. Marković, M. Mičević, 4th Yugoslavian Conference on Metallurgy, Proceedings, Proceedings, 1988.